

# Quantitative PCR Analysis of Functional Genes in Iron-Rich Microbial Mats at an Active Hydrothermal Vent System (Lō'ihi Seamount, Hawai'i)

Kelsey J. Jesser, Heather Fullerton, Kevin W. Hager, Craig L. Moyer

Department of Biology, Western Washington University, Bellingham, Washington, USA

The chemolithotrophic *Zetaproteobacteria* represent a novel class of *Proteobacteria* which oxidize Fe(II) to Fe(III) and are the dominant bacterial population in iron-rich microbial mats. *Zetaproteobacteria* were first discovered at Lō'ihi Seamount, located 35 km southeast off the big island of Hawai'i, which is characterized by low-temperature diffuse hydrothermal venting. Novel nondegenerate quantitative PCR (qPCR) assays for genes associated with microbial nitrogen fixation, denitrification, arsenic detoxification, Calvin-Benson-Bassham (CBB), and reductive tricarboxylic acid (rTCA) cycles were developed using selected microbial mat community-derived metagenomes. Nitrogen fixation genes were not detected, but all other functional genes were present. This suggests that arsenic detoxification and denitrification processes are likely cooccurring in addition to two modes of carbon fixation. Two groups of microbial mat community types were identified by terminal restriction fragment length polymorphism (T-RFLP) and were further described based on qPCR data for zetaproteobacterial abundance and carbon fixation mode preference. qPCR variance was associated with mat morphology but not with temperature or sample site. Geochemistry data were significantly associated with sample site and mat morphology. Together, these qPCR assays constitute a functional gene signature for iron microbial mat communities across a broad array of temperatures, mat types, chemistries, and sampling sites at Lō'ihi Seamount.

Deep-sea hydrothermal vents are dynamic and extremely productive biological ecosystems supported by chemosynthetic microbial primary production. In the absence of photosynthesis, microorganisms derive energy via the oxidation of reduced chemicals [e.g., H<sub>2</sub>, H<sub>2</sub>S, Fe(II), and CH<sub>4</sub>] emitted in hydrothermal fluids (1). In contrast to other strategies for microbial chemosynthesis at hydrothermal vents, iron oxidation has only more recently been studied (2). By weight, iron is the most abundant element in the earth, and it has vast potential as an energy source for microbes via chemolithoautotrophy coupled to Fe(II) oxidation (3). However, iron's ability to act as an electron donor for the biotic fixation of CO<sub>2</sub> in neutrophilic environments is limited by the rapid abiotic oxidation of Fe(II) to Fe(III) in the presence of oxygen (4, 5). Despite the ephemeral nature of iron as an energy source, iron-oxidizing bacteria (FeOB) have been identified in a wide array of freshwater and marine habitats and can flourish at circumneutral deep-sea vents with sharp redox gradients and hydrothermal fluids high in CO<sub>2</sub> and reduced iron (6–9). The recently described *Zetaproteobacteria* represent a novel class of marine *Proteobacteria* that are diverse and abundant contributors to deep-sea FeOB communities (10).

*Zetaproteobacteria* were first discovered at iron-rich, low-temperature hydrothermal vents at Lō'ihi Seamount, HI (2, 11), and have been demonstrated to be significant microbial colonizers of seamounts (10, 12). Lō'ihi Seamount is a seismically active submarine hot spot volcano located approximately 35 km southeast of the big island of Hawai'i. It is the youngest seamount of the Hawaiian Island chain and actively emits Fe(II)- and CO<sub>2</sub>-rich hydrothermal vent effluent, which supports extensive microbial mats (9, 10, 13). In 1996 a major eruption formed Pele's Pit (Fig. 1), a 300-m wide caldera near the summit, with several active hydrothermal venting sites (14).

The *Zetaproteobacteria* appear to have a relatively high pheno-

typic diversity, yet only one species, *Mariprofundus ferrooxydans*, has been described thus far (8, 15, 16). *M. ferrooxydans* is a chemolithoautotrophic microaerophilic FeOB, with few genomic similarities to other hydrothermal vent *Proteobacteria* or other well-characterized freshwater iron oxidizers (16). A recent study analyzed a number of iron-rich microbial biomes in a global survey of small subunit (SSU) rRNA gene sequences and identified 28 unique operational taxonomic units (15). Of these, two were ubiquitous and thereby cosmopolitan throughout the Pacific Ocean. *M. ferrooxydans* was endemic to Lō'ihi, suggesting that *Mariprofundus* sp. strains may be a comparatively minor lineage of *Zetaproteobacteria* from an ecological perspective (10). In addition to *Zetaproteobacteria*, community structure analysis has consistently identified members of the *Gamma*proteobacteria, *Delta*proteobacteria, *Epsilon*proteobacteria, and *Chloroflexi* (15, 17) at Lō'ihi, suggesting additional metabolic and functional diversity within these iron-rich mat communities.

FeOB produce Fe(III)-oxyhydroxides during iron oxidation in

Received 30 October 2014 Accepted 9 February 2015

Accepted manuscript posted online 13 February 2015

Citation Jesser KJ, Fullerton H, Hager KW, Moyer CL. 2015. Quantitative PCR analysis of functional genes in iron-rich microbial mats at an active hydrothermal vent system (Lō'ihi Seamount, Hawai'i). *Appl Environ Microbiol* 81:2976–2984. doi:10.1128/AEM.03608-14.

Editor: G. Voordouw

Address correspondence to Craig L. Moyer, cmoyer@hydro.biol.wvu.edu.

Supplemental material for this article may be found at <http://dx.doi.org/10.1128/AEM.03608-14>.

Copyright © 2015, American Society for Microbiology. All Rights Reserved. doi:10.1128/AEM.03608-14

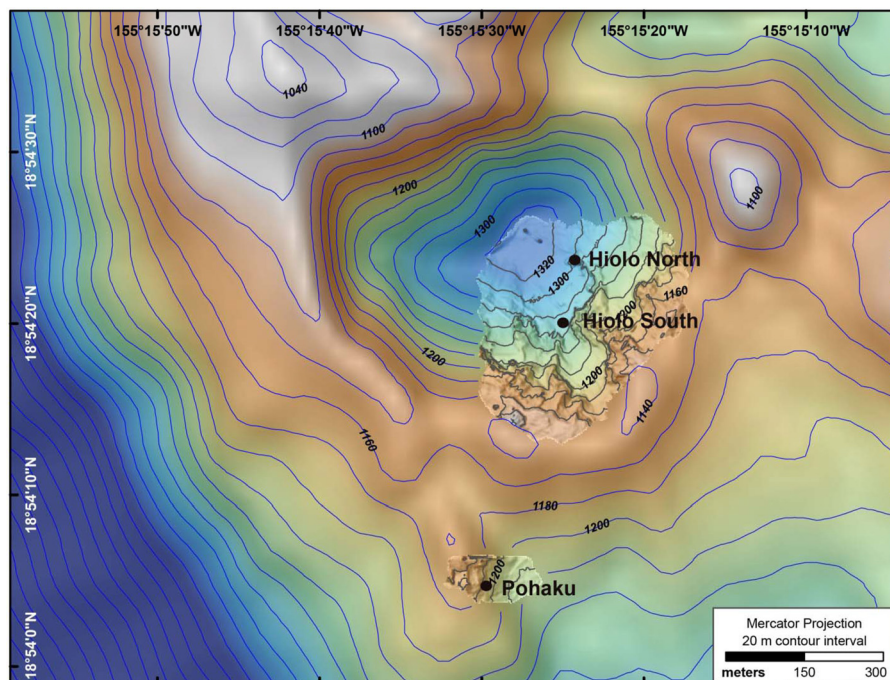


FIG 1 Bathymetric map (including high-resolution overlays) of sampling sites in and on the edge of Pele's Pit at Lō'ihi Seamount, HI. Precise marker locations include Marker 57 at Pohaku, Markers 34 and 38 at Hiolo South, and Markers 31, 36, and 39 at Hiolo North. Courtesy of Susan Merle, NOAA EOI/OSU. (Map created with ArcGIS, version 10.3, software [Esri].)

order to avoid encrustation as Fe(II) is oxidized to insoluble Fe(III) at circumneutral pH (pH 5.5 to 7.4). These structures are instrumental in the formation of microbial mats supplied by Fe(II)-rich vent fluids and are thought to be important in determining fluid flow, dispersion, colonization, and biotic geochemical cycling throughout the ecosystem (18). Distinct mat types associated with various morphologies of Fe(III)-oxyhydroxides (e.g., tubular sheaths versus twisted helical stalks) have been consistently observed at Lō'ihi. Fine-scale microscopy and terminal restriction fragment length polymorphism (T-RFLP) analyses of distinct mat morphotypes (17) provide evidence that various mat types may represent phylogenetically distinct distributions of microbial populations.

To better understand the interplay among the ecologically significant members of these iron-rich mat communities, functional genes were chosen that act as indicators of key steps in both carbon and nitrogen metabolic pathways. RubisCO (ribulose-1,5-bisphosphate carboxylase) is a key enzyme for carbon fixation via the Calvin-Benson-Basham (CBB) cycle. RubisCO type I and II enzymes are most often identified in deep-sea chemolithoautotrophs (19, 20) and have been identified in *M. ferrooxydans*. It has been suggested that these enzymes may be used under various oxygen and carbon dioxide conditions (8, 16) though type II (encoded by *cbmM*) is most effective in high-CO<sub>2</sub> environments (21). ATP citrate lyase (encoded by *acLB*), which catalyzes the ATP-dependent cleavage of citrate, is one of only two enzymes unique to the reductive tricarboxylic acid (rTCA) cycle (22). Though it has been shown that *Zetaproteobacteria* primarily fix carbon through the CBB cycle, other well-known hydrothermal vent organisms, including members of the *Epsilonproteobacteria* and *Aquificales*, are known to use the rTCA cycle (16, 23, 24). Biolog-

ical nitrogen fixation is considered an important potential nitrogen source in hydrothermal systems, and *nifH* sequences have been detected at vents along the Juan De Fuca Ridge (25). Of the genes that encode the three different nitrogenase subunits, *nifH*, which encodes the nitrogenase reductase subunit, is the most commonly used as a molecular marker for microbial nitrogen fixation (26). Nitrite reductase is often used as an indicator for microbial denitrification. The enzyme products (e.g., the product of *nirK*) are responsible for the conversion of nitrite to nitric oxide (or nitrous oxide). This is a key step in denitrification because it reduces mineralized nitrogen and helps differentiate denitrifiers from nitrate respirers (27–30). Finally, the detection of arsenic resistance genes (*arsC*) in our metagenomic assembly from Pohaku Vents represents an exciting opportunity to investigate arsenic detoxification in microbial mat communities at Lō'ihi. This enzyme catalyzes the intracellular reduction of arsenate to arsenite, which is then extruded from the cell via an arsenite-specific protein pump (31, 32). Meyer-Dombard et al. found both *arsC* and *Zetaproteobacteria* SSU rRNA gene sequences in vent fluids and slide colonization experiments in the arsenic-rich waters at shallow hydrothermal vents at Tutum Bay, Papua New Guinea (33).

This study describes the use of five novel, nondegenerate quantitative PCR (qPCR) assays to estimate the abundance of key functional gene sequences for carbon and nitrogen fixation, denitrification, and arsenic detoxification in *Zetaproteobacteria*-rich microbial mat communities at Lō'ihi Seamount, HI. The goal of this research was to use qPCR in conjunction with chemical analyses and T-RFLP DNA fingerprinting to analyze microbial mat samples across a range of environmental parameters. Previous studies have used qPCR to quantify functional genes at hydrother-

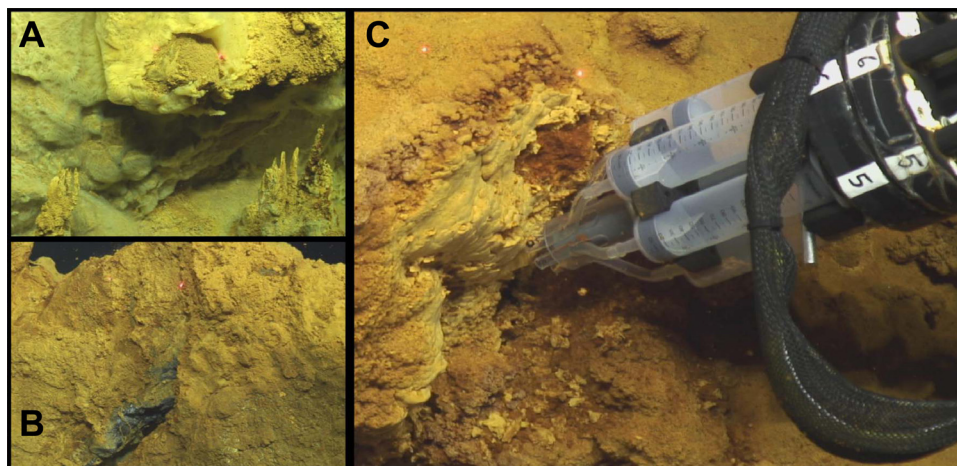


**FIG 2** Microbial iron mats at Lō'ihi Seamount formed by *Zetaproteobacteria* during the oxidation of Fe(II) to insoluble Fe(III) oxyhydroxides at circumneutral pH. The distance between lasers is 10 cm. (A) Iron mats formed over venting chimneys at Hiolo North. The light-colored top layer of the mat, termed veil, has peeled back, revealing the undermat. (B) "Cauliflower" iron mats surrounding an actively venting orifice at Hiolo South. Bacterial streamers can be seen emanating from the vent orifice. (C) The BMS sampler operated by the ROV *Jason II* sampling a curd-like mat layer at Pohaku.

mal vents and in other microbial biomes (34). However, many of these studies have utilized degenerate primers designed using sequence data from databases and other sources. All primers used in this study were either designed or modified to target only the respective functional genes found in metagenomics surveys, thereby focusing on the ecologically significant portion of our mat communities. Our unique approach to nondegenerate primer design for qPCR using sequence data derived from samples collected from these iron-rich microbial mats has enabled us to quantify functional genes specific to these habitats and communities across a wide array of sample sites, chemistries, temperatures, and mat morphologies.

## MATERIALS AND METHODS

**Sampling and DNA extraction for T-RFLP and qPCR.** Microbial iron mat samples were collected within Pele's Pit hydrothermal venting sites, Hiolo North (Markers 31, 36, and 39) and Hiolo South (Markers 34 and 38), and on the caldera rim at Pohaku (Marker 57) at Lō'ihi Seamount, HI (Fig. 1). Samples were collected using a biomat syringe (BMS) sampler, a custom-designed tool for fine-scale microbial mat sampling (35). The BMS sampler was operated by the remotely operated vehicle (ROV) *Jason II* from the research vessel (R/V) *Thomas G. Thompson* during a March 2013 cruise to Lō'ihi. Gross mat morphology was assigned based on consistently observed (unmagnified) mat structures at these sites (Fig. 2). Sample names reflect ROV dive number (671 to 676), sample type and number (BMS1 to BMS3), and the sampler and syringes used (samplers A to D and syringes 1 to 6; e.g., B123456). For comparison, a single scoop sample, PV340, was also included. This sample was collected in 1997 using the deep submergence rescue vehicle (DSRV) *Pisces V* at Jet Vents (Marker 11). This location is no longer active, and the mat community was not indicative of an FeOB-dominated mat community but, rather, was dominated exclusively by populations of known sulfur-cycling *Epsilonproteobacteria*. Mat samples were brought onboard and either frozen at  $-80^{\circ}\text{C}$  or directly extracted for genomic DNA (gDNA). Extractions were done using a FastDNA spin kit for soil (Qbiogene, Carlsbad, CA) according to the manufacturer's protocol. A FastPrep instrument (Qbiogene) was used at speed 5.5 for 45 s to optimize cellular lysis, and gDNA was then eluted in 10 mM Tris at pH 8.0. A NanoDrop ND-1000 spectrophotometer (Nano-

Drop, Wilmington, DE) was used to determine the purity and concentration of all nucleic acid samples.

**Metagenomic sequencing and assembly.** Two previously collected samples were used to verify qPCR primer design. Syringe sample J2-479-BS3 (81.8% *Zetaproteobacteria* by qPCR) was collected from a microbial iron mat at Pohaku (Fig. 1) in 2009 using the ROV *Jason II*. Scoop sample SB13 (13% *Zetaproteobacteria*) was collected in 2011 directly from an intertidal microbial iron mat at site 13, Soda Bay, AK, and immediately preserved with RNAlater. A HiSeq Illumina platform was used for sequencing gDNA (extracted as described above) from these samples. Reads were assembled using MetaVelvet, a freeware short-read assembler for metagenomics (36). Genes of interest were identified using MG-RAST annotations of metagenome assemblies (37).

**Primer design.** Nondegenerate qPCR primers for arsenate reductase (*arsC*) and nitrite reductase (*nirK*) were designed using annotated functional gene sequences from our Pohaku (J2-479-BS3) metagenomic assembly. Nitrogenase was not detected in the Pohaku metagenomics assembly. Therefore, *nifH* primers were based on an annotated functional gene sequence from the SB13 metagenomic assembly. Five sets of commonly used degenerate *nifH* primers (26) were also tested against Lō'ihi 2013 BMS samples, with no amplification (data not shown). Nondegenerate qPCR primers were designed for carbon fixation genes using PCR-cloned sequences. PCR primers for ribulose-1,5-bisphosphate carboxylase (RubisCO) type II (*cbmM*) and ATP citrate lyase (*aclB*) genes were first obtained from previous studies (38, 39). These degenerate primer sets for *cbmM* and *aclB* were used to amplify and sequence PCR products from Lō'ihi 2013 BMS samples. Sequence data for PCR-cloned amplicons were used to generate nondegenerate nested primer sets for qPCR that are specific for the microbial communities at Lō'ihi (Table 1). Nearly complete bacterial and *Zetaproteobacteria* SSU rRNA gene sequences from the NCBI database were aligned with the SILVA SINA web aligner (40) and imported into the SILVA, version 102, nonredundant (NR) database using ARB (41).

**Cloning for qPCR standards.** PCRs were performed with 3 ng of gDNA template using a reaction mixture containing 1  $\mu\text{M}$  each forward and reverse primer, 2.5 mM MgCl<sub>2</sub>, 1  $\mu\text{M}$  Taq, 1 $\times$  PCR buffer, 10  $\mu\text{g}$  of bovine serum albumin (BSA), and 200  $\mu\text{M}$  each deoxynucleoside triphosphate (dNTP). Thermocycling consisted of an initial 2-min hot start at 94 $^{\circ}\text{C}$ , 35 cycles of 94 $^{\circ}\text{C}$  for 1 min, 50 to 60 $^{\circ}\text{C}$  for 90 s, and 72 $^{\circ}\text{C}$  for 3 min, with a final elongation step at 72 $^{\circ}\text{C}$  for 3 min. Annealing temperature varied for each primer set (Table 1). PCR products were examined by

TABLE 1 Summary of qPCR primers

Gene product or region (symbol)	Function	Primer	Primer sequence (5'–3')	Source or reference for qPCR primer sequence	Annealing temp (°C)
Nitrogenase ( <i>nifH</i> )	Nitrogen fixation	nifH5F	GGTAAATCCACTACTACCCAGAA	Soda Bay, AK, Illumina assembly	55
		nifH5R	GAAGGATCAGACGTGTGGAA		
Nitrite reductase ( <i>nirK</i> )	Denitrification	nir2F	CGTGCATAATAACGGTGAT	Lō'ihī, HI, Illumina assembly	60
		nir2R	CCTTCTGCCAATGGTCCTT		
Arsenate reductase ( <i>arsC</i> )	Arsenic detoxification	arsC2F	GCGTACAGGCGAAGATGAATA	Lō'ihī, HI, Illumina assembly	60
		arsC2R	ACAACAACAGGACGTCAA		
ATP citrate lyase ( <i>aclB</i> )	Carbon fixation via rTCA cycle	aclB3F	GCTTTGGCAAATGGTTCAGG	Amplicons derived using degenerate primers (39)	53
		aclB3R	ACCGACTTCTGGAAAGTATTGG		
RubisCO type II ( <i>cbmM</i> )	Carbon fixation via CBB cycle	cbmM7.3F	GCTTTGGCAAATGGTTCAGG	Amplicons derived using degenerate primers (38)	60
		cbmM7.3R	ACCGACTTCTGGAAAGTATTGG		
SSU rRNA	Ribosome	Zeta542F	GAAAGGDGCAAGCGTTGTT	Lō'ihī SSU libraries (15)	60
SSU rRNA	Ribosome	Zeta658R	TGCTACACDCGGAATCCGC	Lō'ihī SSU libraries (15)	60
		Bact533F	GTGCCAGCAGCCGCGGTAA		
		Bact684R	TCTACGSATTTYACYSCTAC		

electrophoresis on a 2% agarose gel in 1× Tris-acetate-EDTA (TAE) buffer. PCR products were purified using a QIAEX II gel extraction kit (Qiagen, Valencia, CA) according to the manufacturer's protocol.

Cleaned PCR amplicons were cloned into the pCR4-TOPO *Escherichia coli* vector using a TOPO TA cloning kit for sequencing with One Shot TOP10 chemically competent cells according to the manufacturer's instructions (Life Technologies, Carlsbad, CA). Randomly selected colonies were streaked to isolation and then inoculated into 5 ml of LB broth at 37°C in a shaking incubator overnight. Plasmids were extracted and purified from cloned cells using a QIAprep miniprep system (Qiagen) and PCR screened for correct insert size using the M13F and M13R primers (42). PCR products were examined by electrophoresis on a 2% agarose gel in TAE buffer.

Cloned amplicons were sequenced with M13F and M13R primers with an ABI 3130xl genetic analyzer (Life Technologies). Forward and reverse sequences were aligned and trimmed using BioNumerics, version 7.1 (Applied Maths, Sint-Martens-Latem, Belgium). Cloned sequences were analyzed to ensure the correct target for hybridization. All plasmid standards were linearized for use in qPCR assessments using the restriction enzyme NotI (New England BioLabs).

**qPCR and T-RFLP analysis.** qPCR amplifications were performed in triplicate using a Step One Plus real-time PCR system (Life Technologies). Reaction mixtures (20 µl final volume) contained 10 µl of 2× Power SYBR green master mix (Life Technologies), forward and reverse primers (0.3 µM each), and 1 ng of template DNA. Cycling conditions were 95°C for 10 min and 40 cycles of 95°C for 15 s and 50 to 60°C for 1 min, followed by melting curve analysis from 60 to 95°C. Total gene copy numbers were determined by analyzing a dilution series of a known quantity of plasmid containing the gene of interest (see above) as determined with a Nano-Drop spectrophotometer. Standard curves and linear regression data for each assay were calculated, as well as standard deviation for each range of cycle threshold ( $C_T$ ) values produced. Gene copy number per nanogram of gDNA was determined based on the size of the linearized plasmid used as the qPCR standard (43). Percent *Zetaproteobacteria* was calculated by dividing *Zetaproteobacteria* gene copy numbers per nanogram of gDNA by copy numbers calculated against the bacterium-specific primer set (17). No qPCR data were used unless primers exhibited better than 95% efficiency and yielded single-peak amplicons upon post-PCR melt curve analysis.

PCR amplification and digestion for T-RFLP were performed as previously described (44). Community fingerprints were compared using average Pearson product moment correlation and unweighted pair group method with arithmetic mean (UPGMA) cluster analysis for all eight di-

gests using the relative fluorescent proportions of each electropherogram. Cophenetic correlation coefficient values were calculated for all nodes with three or more branches.

**Chemistry and temperature measurements.** End-member hydrothermal fluids were collected from chimneys and microbial mats using a titanium major sampler deployed from the ROV *Jason II* (45). Background samples were collected away from venting sites using Niskin bottles attached to the side of ROV *Jason II*. Hydrothermal fluid samples were filtered through 0.2-µm-pore-size polycarbonate filters and then frozen immediately.

Fluid temperatures were measured using the temperature probe on ROV *Jason II*.  $\text{NO}_x$  ( $\text{NO}_2$  plus  $\text{NO}_3$ ) was measured using the chemiluminescent method with a  $\text{NO}_x$  box, which has a detection limit of <0.010 µM  $\text{NO}_x$  (46, 47).  $\text{NH}_4^+$  was measured using the fluorescence method (47) postcruise. The detection limit for  $\text{NH}_4^+$  is 0.030 µM. Dissolved inorganic phosphorus ( $\text{P}_i$ ) and dissolved silica (mostly silicate; dSi) were measured using colorimetric methods, with detection limits of 0.030 µM  $\text{P}_i$  and 0.30 µM dSi (48). Fe(II) concentrations in mat samples were determined using the ferrozine method with a detection limit of <1 µM (49).

**Statistical analyses.** A nonparametric Kruskal-Wallis one-way analysis of variance (ANOVA) was run for all functional gene qPCR data using the program SigmaPlot, version 12.5 (Systat Software, San Jose, CA). A nonparametric multidimensional scaling (NMDS) plot was created between variables for log-transformed functional gene qPCR data and *Zetaproteobacteria* abundance qPCR data using a Pearson product correlation resemblance matrix using Primer, version 6 (50). *nifH* gene amplification was low or undetectable by our method and was not included in the NMDS plot.

Four nonparametric one-way multivariate analyses of variance (MANOVA) were run for qPCR gene abundance numbers (*cbmM*, *aclB*, *arsC*, *nirK*, and *nifH*) for the following independent variables: mat morphology, temperature range (10°C intervals), percent *Zetaproteobacteria* range (5 to 10% intervals), and sample site. Three one-way MANOVA were run for chemistry data with the independent variables of mat morphology, temperature range, and sample site. Wilks' lambda  $P$  values below 0.05 were considered statistically significant. For significant results, tests between subject effect (univariate ANOVA) results were examined to determine which variables were statistically significant for a given independent variable ( $P < 0.05$ ). These analyses were completed using the statistical software SPSS, version 17 (IBM, Armonk, NY).

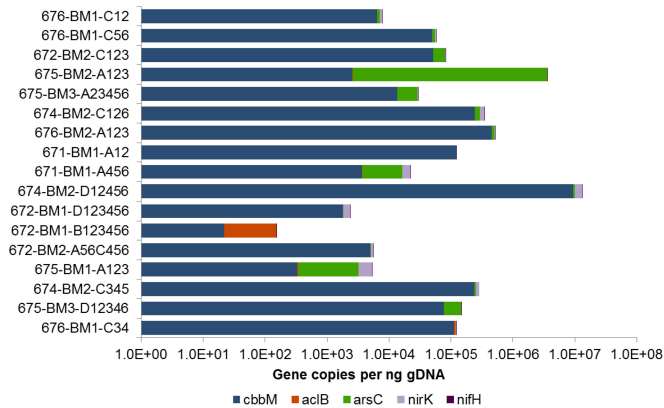


**FIG 3** Stacked bar graphs showing functional gene copy numbers by qPCR for *cbbM*, *acIB*, *arsC*, *nirK*, and *nifH* for 17 BMS samples collected at Lō'ihi in 2013. Functional gene copy numbers are represented on a logarithmic ordinate.

**RESULTS**

qPCR analysis for 17 Lō'ihi 2013 samples across various mat morphologies, temperatures, fluid chemistries, and sample sites revealed unique functional gene signatures for each fine-scale microbial mat community sampled by the BMS sampler (Fig. 3). As expected, there was substantial variation in functional gene abundances across communities. Overall, the Calvin-Benson-Bassham (CBB) carbon fixation gene *cbbM* was the most abundant gene sequence, followed by *arsC*, *nirK*, and *acIB*, based on cumulative averages. Gene copy numbers for *nifH* were either very low or undetectable by our method. Two mat samples from Hiolo South (675-BM2-A123 and 675-BM1-A123) had relatively high *arsC* copy numbers and came from sites that were >40°C (upper end of the sampled temperature range). Pohaku sample 674-BM2-D12456 had the greatest number of cumulative gene copy numbers across the five qPCR assays (>10<sup>7</sup>). Hiolo North sample 672-BM1-B123456 had the fewest gene copy numbers (<10<sup>3</sup>) and had high *acIB* gene copy numbers per nanogram of gDNA relative to the other mat samples. Nonparametric Kruskal-Wallis one-way ANOVA showed that differences in the median abundances between functional genes were greater than would be expected by chance (*P* < 0.001). The nonparametric multidimensional scaling (NMDS) plot (Fig. 4) for qPCR functional gene variables and for *Zetaproteobacteria* abundance clustered *cbbM*, *nirK*, and *arsC*, with >60% Pearson correlation coefficient similarity. This group was also associated with *Zetaproteobacteria* abundance. *acIB* did not group with any other qPCR variable.

T-RFLP DNA fingerprinting (Fig. 5A) revealed that the microbial communities at hydrothermal vents near the summit region of Lō'ihi Seamount were very similar to each other (>40% similarity between samples). T-RFLP clusters were assigned membership in two distinct groups. T-RFLP group 1 had 33% *Zetaproteobacteria* on average and low *acIB* abundance relative to that of group 2. T-RFLP group 2 had 9.1% *Zetaproteobacteria* and much higher *acIB* copy numbers and was grouped more closely with the comparator sample PV340 (*Zetaproteobacteria* were only just detectable at 0.21% in this sample). Pohaku BMS samples were all clustered in T-RFLP group 1. Hiolo North and Hiolo South samples formed distinct clusters within group 1 according to vent type and temperature although 672-BM1-D123456, a Hiolo North curd-like mat, grouped more closely with the Pohaku mat sam-

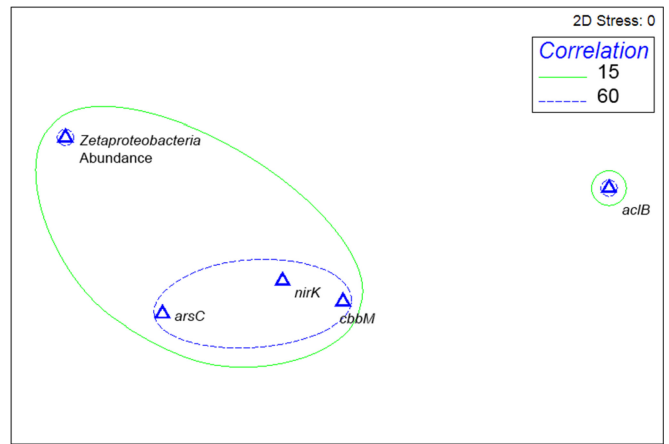


**FIG 4** Pearson correlation nonparametric multidimensional scaling (NMDS) plot generated using a group average resemblance matrix of log-transformed functional gene and *Zetaproteobacteria* abundance qPCR data for 17 BMS samples. Contours indicate clusters with 15 and 60% Pearson correlations. 2D, two-dimensional.

ples. Two veil-type samples from different sites (672-BM1-B12345 and 672-BM2-A56C456) clustered tightly, with >80% similarity in the community fingerprint analysis. Clustering for group 2 (based solely upon T-RFLP data) was comprised of two Hiolo South samples, 675-BM3-D12346 (surface mat; 48.1°C) and 676-BM2-C34 (streamers; 33.1°C).

Functional gene data for key carbon fixation enzymes encoded by *acIB* (Fig. 5B) and *cbbM* (Fig. 5C) were compared with the T-RFLP community analysis (Fig. 5A). Sample PV340 had very high *acIB* gene copy numbers relative to those of the Lō'ihi 2013 BMS samples. Group 2 was most closely associated with PV340, and group 1 samples had relatively low *acIB* gene copy numbers compared to those of group 2 and PV340. Both PV340 and 676-BM2-C34 are classified as streamers, filament-like mats in actively venting orifices (Fig. 2B). Overall, samples low in *acIB* generally had much higher abundance of *cbbM*, which was ubiquitous in all samples.

Geochemical measurements were collected for 14 of our 17 Lō'ihi BMS samples (see Table S1 in the supplemental material). Mat morphology and site location were significantly associated (see Table S2) with vent chemistry (one-way MANOVA, *P* < 0.0005 for both). Mat temperature was not significantly associated with any chemistry measure (one-way MANOVA, *P* = 0.087). Univariate ANOVA showed that Fe(II) levels were significantly associated with mat type (*P* = 0.003) and that NH<sub>4</sub>, NO<sub>3</sub>, dSI, and PO<sub>4</sub> were significantly associated with site (*P* = 0.019, 0.030, 0.001, and <0.0005, respectively) (see Table S3 in the supplemental material).

One-way MANOVA for functional gene qPCR data indicated that mat morphology was a significant factor for qPCR variance across samples (*P* < 0.0005). Temperature, sample site, and percent *Zetaproteobacteria* did not significantly describe the variation in qPCR data (see Table S2 in the supplemental material). Univariate ANOVA revealed that *acIB* gene copy numbers were significantly explained by changes in mat type (*P* < 0.0005). Functional gene abundances for *cbbM*, *arsC*, *nirK*, and *nifH* were not significantly associated with mat morphology (see Table S4).

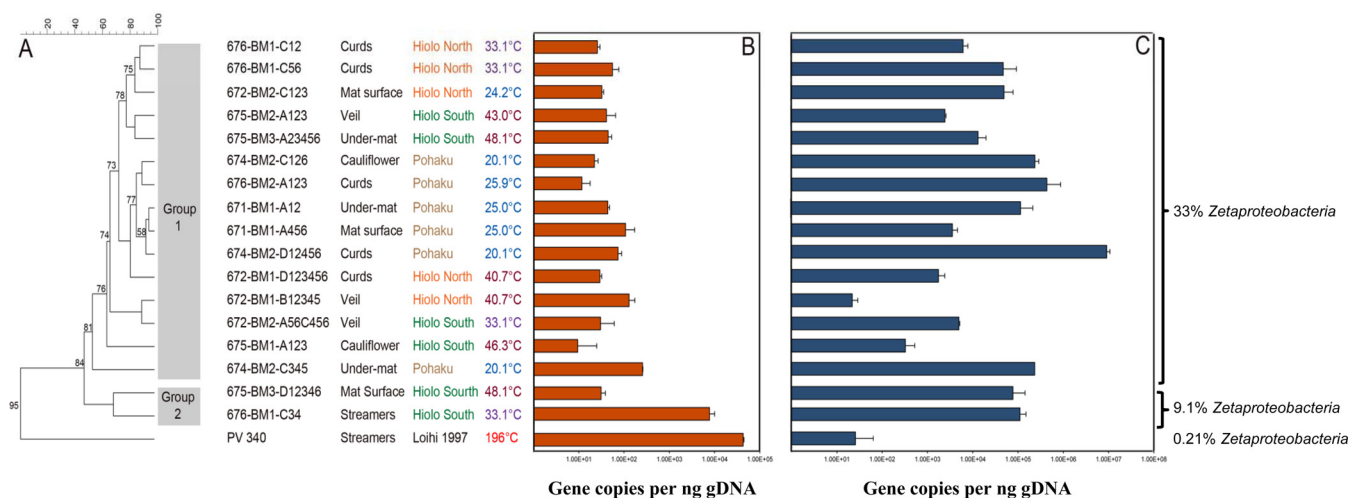


FIG 5 (A) Group-average cluster analysis of T-RFLP DNA fingerprints from 17 Lō'ihi BMS samples. PV340, a 1997 scoop sample taken shortly after a major eruption event at Lō'ihi, is included for comparison. Cophenetic correlation coefficient values are at nodes with three or more branches. (B) Bar graph showing *acdB* gene copy numbers per nanogram of gDNA. (C) Bar graph showing *cbbM* gene copy numbers per nanogram of gDNA. Error bars represent standard errors across triplicate qPCRs. Functional gene copy numbers are represented on a logarithmic ordinate.

## DISCUSSION

These novel qPCR assays were designed to target annotated gene sequences from microbial mats at Lō'ihi Seamount vent sites. Because our primers are nondegenerate, we have enhanced confidence in the sequence identity of the PCR amplicons. We are reporting on the amplification of functional genes via primers designed to target sequences unambiguously identified in microbial communities at our study sites. Most qPCR approaches to functional gene amplification in environmental samples have utilized degenerate primers and have largely focused on the amplification of one or two genes associated with a single pathway or group of organisms (51–53). Use of degenerate primers increases the risk of nonspecific amplification, largely due to primer bias (54). As qPCR is an exceptionally sensitive molecular tool, we chose to be conservative in our strategy for probe design, using either annotated metagenomic functional gene sequences or cloned sequence representatives of microbial mat communities present at Lō'ihi to design primers (Table 1).

Bacterial arsenic resistance and detoxification are conferred by *arsC*. We found that *arsC* is present and quantifiable in all iron-rich mat communities assayed (Fig. 3). Though there is presently no data on arsenate/arsenite chemistry at Lō'ihi, a previous study found both *arsC* and *Zetaproteobacteria* SSU gene sequences in arsenic-rich vent fluids (33). We identified several samples high in *arsC* that are intriguing candidates for continued investigations into the presence and expression of arsenic cycling genes. Two samples (675-BM2-A123 and 675-BM1-A123) had exceptionally higher *arsC* genes present than the other Lō'ihi 2013 mat communities analyzed. In the absence of measurements for arsenic geochemistry, it is difficult to speculate on why these two samples have elevated *arsC* gene copy numbers when other samples from Hiolo South did not. However, the difference may have to do with our ability for fine-scale sampling of mats at a diffuse vent site and/or the ephemeral nature of exposure to vent effluent.

Nitrogen fixation via *nifH* is the most commonly used molecular marker for nitrogen fixation (26). However, amplification of *nifH* using a wide array of both degenerate and nondegenerate

primer sets resulted in no detection (data not shown), nor was *nifH* detected in the Pohaku metagenome assembly. Therefore, we developed an assay to quantify nitrogenase (*nifH*) identified from a *Zetaproteobacteria*-rich iron seep at Soda Bay, AK. Still, gene abundance of *nifH* was estimated to be either very low or undetectable in the Lō'ihi mat communities that were analyzed. It is possible that nitrogen fixation via *nifH* is not an important function of hydrothermal iron-based microbial mat communities even though it has been found in subsurface hydrothermal vent habitats from the Juan de Fuca Ridge, where comparable levels of fixed nitrogen were measured (25).

The presence of a dissimilatory copper-containing nitrite reductase (*nirK*) at Lō'ihi is suggestive of denitrifying activity. Often used as a molecular probe for microbial denitrification, *nir*-encoded enzymes are responsible for reducing a mineralized form of nitrogen to a gaseous form (27–30). Though previous studies have identified denitrification genes at hydrothermal vents (34, 55, 56), they were only recently detected at Lō'ihi and in at least some *Zetaproteobacteria* as well via an annotated metagenomic assembly of a fosmid library (57). The presence of *nirK* was detected in all mat samples described here, confirming the presence of denitrification genes in a wide array of iron mat communities. The presence of *nirK* is notable as nitrite reduction may open up new ecological niches for microorganisms within iron-rich mat habitats, with nitrogen oxides acting as electron acceptors in lieu of oxygen. Amplification of a major *nirK* gene across all samples indicates the capacity for denitrification and may expand the habitat range of *Zetaproteobacteria* to anoxic habitats containing nitrite.

The CBB cycle is thought to be the most prevalent mode of carbon fixation on earth and often occurs at hydrothermal vents (19). RubisCO proteins are organized into four groups, with type I (encoded by *cbbL*) and type II (encoded by *cbbM*) most often identified in deep-sea chemolithoautotrophs (19, 20, 58). A dimer of large subunits, the protein encoded by *cbbM* is considered most effective in higher-carbon dioxide environments (21). High levels of CO<sub>2</sub> (>300 mM) have been detected in vent effluents at Lō'ihi

(59), and metagenomic assemblies (data not shown) from Lō'ihi mats have shown that *cbbM* is much more prevalent than *cbbL*. The ubiquity of *cbbM* in the 17 fine-scale mat communities collected with the BMS sampler and assayed here (Fig. 3 and 5C) suggests that the CBB cycle via *cbbM* is likely the most important mode of carbon fixation in this habitat. Both *cbbL* and *cbbM* have been identified in *M. ferrooxydans* (8, 16). Future culturing endeavors should focus on the communities high in *cbbM* using enrichments with elevated CO<sub>2</sub> in an attempt to isolate the more ecologically relevant *Zetaproteobacteria*, which have an extremely broad biogeographic distribution (15).

The reductive tricarboxylic acid (rTCA) cycle represents another mode of carbon fixation found at hydrothermal vents that can be characterized with ATP citrate lyase (encoded by *aclB*) (19, 23, 60). *M. ferrooxydans* does not have *aclB* (16). Other known hydrothermal vent microorganisms, including well-characterized members of the *Epsilonproteobacteria* and *Aquificales*, are known to utilize the rTCA cycle and have been identified at Lō'ihi (16, 23, 24, 60). *aclB* was much less abundant than *cbbM* in our 17 BMS samples (Fig. 3 and 5B and C), suggesting that, while the gene sequence for *aclB* is present at Lō'ihi, the rTCA cycle is not as widely used as the CBB cycle. As the rTCA cycle operates in the *Epsilonproteobacteria* and generally at higher-temperature deep-sea vents, the abundance of *cbbM* relative to that of *aclB* supports the hypothesis that although *aclB* genes are present, *Zetaproteobacteria* at Lō'ihi use the CBB cycle as their primary means of carbon fixation (10, 23, 38).

Scoop sample PV340 was collected just after the 1996 eruption at a now dormant hydrothermal venting site (maximum temperature [ $T_{\max}$ ] of 196°C). At this time, the microbial mats within and around Pele's Pit were characterized by much higher temperatures and sulfur-dependent microbial communities. This sample exhibited high *aclB*, low *Zetaproteobacteria*, and low *cbbM* abundances relative to iron-rich samples collected in 2013 (Fig. 5B and C). Based on T-RFLP data, the PV340 sample represents a very different community than any of the 2013 Lō'ihi iron mats (Fig. 5A). This observation is consistent with temporal changes in microbial community composition at seamounts and gradual shifts from *Epsilonproteobacteria*-dominated communities to *Zetaproteobacteria*-dominated communities as vents cool and become more diffuse over time (10). A Lō'ihi 2013 streamer sample (676-BM1-C34) was contained in the T-RFLP cluster (group 2) nearest to PV340 and had high *aclB* copy numbers. This hypothesis is reinforced by *Zetaproteobacteria* abundance data; we found that the group 1 cluster had an average of 33% *Zetaproteobacteria*, whereas the group 2 cluster had only 9.1% *Zetaproteobacteria*. The posteruption microbial mat sample PV340 had only 0.21% *Zetaproteobacteria*, further suggesting that the percentage of *Zetaproteobacteria* present is inversely associated with *aclB*. Both *Zetaproteobacteria* abundance and *aclB* gene copy numbers affect the observed community structure transitions since T-RFLP clustering is influenced by mat morphology and since there is a statistically significant relationship between *aclB* copy numbers and mat morphology (univariate ANOVA,  $P < 0.0005$ ).

Geochemistry data were significantly correlated with mat morphology, suggesting that the chemistry of the mat environment is important for determining mat morphology. Fe(II) levels were also significantly correlated by mat type; thus, ferrous iron availability is also likely an important factor for determining mat morphology. As variance in the abundances of the five target genes was

significantly associated with mat type via a one-way MANOVA, Fe(II) may also play a role in variation across functional gene abundances (see Table S2 in the supplemental material). This is unsurprising given the vital role of iron as an electron donor in the mat habitats at Lō'ihi. qPCR-measured abundances for *cbbM*, *arsC*, *nirK*, and *nifH* were not associated with any independent variable in the univariate ANOVA, suggesting that these functional genes are not affected by vent temperature or site (see Table S4). Conversely, *aclB* gene copy numbers were significantly affected by mat type, supporting the idea that this gene may be another good indicator of community composition. Morphology was significant with Fe(II) concentrations in the mats, leading us to hypothesize that reduced iron availability is a forcing function for functional gene abundances, community composition, and mat type.

Locations of the vents are important for some chemical factors, as seen by the significant relationship between sample site and amount of NH<sub>4</sub>, NO<sub>x</sub>, dSi, and PO<sub>4</sub> (see Table S3 in the supplemental material). This relationship between sample site and geochemistry was not reflected in the qPCR data. Changes in gene abundance occur gradually, while chemical changes in the vent environment may happen rapidly; and it is likely that the microorganisms living in ephemeral habitats are able to function within a range of chemistries. There was no detectable effect of temperature on geochemistry or qPCR data. This is likely due to the relatively narrow temperature range (20 to 50°C) of iron-dominated microbial mat communities.

An NMDS plot was created for the qPCR functional gene data (except *nifH*) and *Zetaproteobacteria* abundance using a Pearson correlation resemblance matrix (Fig. 4). The NMDS analysis grouped *cbbM*, *nirK*, and *arsC* functional genes together. These genes loosely clustered with *Zetaproteobacteria* abundance, indicating that *Zetaproteobacteria* within the community affect the abundance of these functional genes. Both *nirK* and *cbbM* have been identified in PV-1 as well as in other uncharacterized strains of *Zetaproteobacteria* (16, 57). Arsenic species have been associated with Fe(III) iron-oxhydroxides, such as those formed by *Zetaproteobacteria* at Lō'ihi, in both shallow and deep-sea hydrothermal vent systems (61–63). The rTCA cycle gene *aclB* did not cluster with any other qPCR variable (*arsC*, *nifH*, *nirK*, or *cbbM*). This is unsurprising as it is widely accepted that the rTCA cycle is not associated with *Zetaproteobacteria* but with other taxa at vents, such as the *Epsilonproteobacteria* and *Aquificales* (16, 24). T-RFLP group 2 and corresponding *aclB* abundances at Lō'ihi may also be indicators of community structure; they are not associated with the greater *Zetaproteobacteria*-impacted microbial communities. Comparison of *cbbM* and *aclB* gene abundances revealed that while *cbbM* was ubiquitous in the iron-rich microbial mat habitats, *aclB* was present at appreciable amounts only in the *Epsilonproteobacteria*-rich PV340 and group 2 cluster of mat communities.

qPCR can be utilized to efficiently screen large numbers of samples for distinctive functional gene patterns in ecological contexts (53, 64). The cumulative result of these five qPCR assays is the construction of a unique functional gene signature for discrete, fine-scale microbial mat communities (Fig. 3). These functional gene signatures can be compared across a broad range of environmental parameters and can be used to identify exceptional samples for culturing efforts or additional molecular analyses. The five assays we developed can potentially be used in the continued

study of the functional capacities of iron-dominated hydrothermal communities. qPCR is also a sensitive molecular tool that is best used in conjunction with other assessments and measures, such as the community structure and chemical analyses presented here. This study demonstrates the use of environmentally derived sequence data to design habitat-specific nondegenerate qPCR assays. When combined with phylogenetic and geochemical analyses, this approach gives strong insights into community dynamics and functions and can be applied across a variety of microbial communities and in a wide range of ecosystems.

## ACKNOWLEDGMENTS

We thank the operation team of the ROV *Jason II* and the crew of the R/V *Thomas G. Thompson* for their assistance with sample collection during our March 2013 cruise to Hawai'i. We acknowledge the collaboration of Brian Glazer and Jason Sylvan and thank them for performing the chemical measurements reported here. We also thank the undergraduate researchers in the Moyer lab who helped run T-RFLP analyses and PCRs and contributed to sequencing, especially Jessie Kimber and Tristan Hilton.

This work was funded in part by Western Washington University's Office of Research and Sponsored Programs, by the Biology Alumni Student Research Fellowship, and by the National Science Foundation, award OCE 1155756 (to C.L.M.).

## REFERENCES

- Jannasch HW, Mottl MJ. 1985. Geomicrobiology of deep-sea hydrothermal vents. *Science* 229:717–725. <http://dx.doi.org/10.1126/science.229.4715.717>.
- Emerson D, Moyer CL. 2002. Neutrophilic Fe-oxidizing bacteria are abundant at the Loihi Seamount hydrothermal vents and play a major role in Fe oxide deposition. *Appl Environ Microbiol* 68:3085–3093. <http://dx.doi.org/10.1128/AEM.68.6.3085-3093.2002>.
- Hedrich S, Schlömann M, Johnson DB. 2011. The iron-oxidizing proteobacteria. *Microbiology* 157:1551–1564. <http://dx.doi.org/10.1099/mic.0.045344-0>.
- Weber KA, Achenbach LA, Coates JD. 2006. Microorganisms pumping iron: anaerobic microbial iron oxidation and reduction. *Nat Rev Microbiol* 4:752–764. <http://dx.doi.org/10.1038/nrmicro1490>.
- Druschel GK, Emerson D, Sutka R, Suchecki P, Luther GW, III. 2008. Low-oxygen and chemical kinetic constraints on the geochemical niche of neutrophilic iron(II) oxidizing microorganisms. *Geochim Cosmochim Acta* 72:3358–3370. <http://dx.doi.org/10.1016/j.gca.2008.04.035>.
- Sobolev D, Roden EE. 2004. Characterization of a neutrophilic, chemolithoautotrophic Fe(II)-oxidizing  $\beta$ -proteobacterium from freshwater wetland sediments. *Geomicrobiol J* 21:1–10. <http://dx.doi.org/10.1080/01490450490253310>.
- Holland HD. 2006. The oxygenation of the atmosphere and oceans. *Philos Trans R Soc Lond B Biol Sci* 361:903–915. <http://dx.doi.org/10.1098/rstb.2006.1838>.
- Emerson D, Rentz JA, Lilburn TG, Davis RE, Aldrich H, Chan C, Moyer CL. 2007. A novel lineage of *Proteobacteria* involved in formation of marine Fe-oxidizing microbial mat communities. *PLoS One* 2:e667. <http://dx.doi.org/10.1371/journal.pone.0000667>.
- Glazer BT, Rouxel OJ. 2009. Redox speciation and distribution within diverse iron-dominated microbial habitats at Loihi Seamount. *Geomicrobiol J* 26:606–622. <http://dx.doi.org/10.1080/01490450903263392>.
- Emerson D, Moyer CL. 2010. Microbiology of seamounts: common patterns observed in community structure. *Oceanography* 23:148–163. <http://dx.doi.org/10.5670/oceanog.2010.67>.
- Moyer CL, Dobbs FC, Karl DM. 1995. Phylogenetic diversity of the bacterial community from a microbial mat at an active, hydrothermal vent system, Loihi Seamount, Hawaii. *Appl Environ Microbiol* 61:1555–1562.
- Rassa AC, McAllister SM, Safran SA, Moyer CL. 2009. *Zeta-Proteobacteria* dominate the colonization and formation of microbial mats in low-temperature hydrothermal vents at Loihi Seamount, Hawaii. *Geomicrobiol J* 26:623–638. <http://dx.doi.org/10.1080/01490450903263350>.
- Sakai H, Tsubota H, Nakai T, Ishibashi J, Akagi T, Gamo T, Tilbrook B, Igarashi G, Kodera M, Shitashima K, Nakamura S, Fujioka K, Watanabe M, McMurtry M, Malahoff A, Ozima M. 1987. Hydrothermal activity on the summit of Loihi Seamount, Hawaii. *Geochem J* 21:11–21. <http://dx.doi.org/10.2343/geochemj.21.11>.
- Duennebiek FK, Becker NC, Caplan-Auerbach J, Clague DA, Cowen J, Cremer M, Garcia M, Goff F, Malahoff A, McMurtry G, Midson BP, Moyer CL, Norman M, Okubo P, Resing JA, Rhodes JM, Rubin K, Sansone FJ, Smith JR, Spencer K, Wen X, Wheat CG. 1997. Researchers rapidly respond to submarine activity at Loihi volcano, Hawaii. *Eos* 78:229–233. <http://dx.doi.org/10.1029/97EO00150>.
- McAllister SM, Davis RE, McBeth JM, Tebo BM, Emerson D, Moyer CL. 2011. Biodiversity and emerging biogeography of the neutrophilic iron-oxidizing *Zetaproteobacteria*. *Appl Environ Microbiol* 77:5445–5457. <http://dx.doi.org/10.1128/AEM.00533-11>.
- Singer E, Emerson D, Webb EA, Barco RA, Kuenen JG, Nelson WC, Chan CS, Comolli LR, Ferreira S, Johnson J, Heidelberg JF, Edwards KJ. 2011. *Mariprofundus ferrooxydans* PV-1 the first genome of a marine Fe(II) oxidizing *Zetaproteobacterium*. *PLoS One* 6:e25386. <http://dx.doi.org/10.1371/journal.pone.0025386>.
- Fleming EJ, Davis RE, McAllister SM, Chan CS, Moyer CL, Tebo BM, Emerson D. 2013. Hidden in plain sight: discovery of sheath-forming, iron-oxidizing *Zetaproteobacteria* at Loihi Seamount, Hawaii, USA. *FEMS Microbiol Ecol* 85:116–127. <http://dx.doi.org/10.1111/1574-6941.12104>.
- Chan CS, Fakra SC, Emerson D, Fleming EJ, Edwards KJ. 2011. Lithotrophic iron-oxidizing bacteria produce organic stalks to control mineral growth: implications for biosignature formation. *ISME J* 5:717–727. <http://dx.doi.org/10.1038/ismej.2010.173>.
- Nakagawa S, Takai K. 2008. Deep-sea vent chemoautotrophs: diversity, biochemistry and ecological significance. *FEMS Microbiol Ecol* 65:1–14. <http://dx.doi.org/10.1111/j.1574-6941.2008.00502.x>.
- Shively JM, van Keulen G, Meijer WG. 1998. Something from almost nothing: carbon dioxide fixation in chemoautotrophs. *Annu Rev Microbiol* 52:191–230. <http://dx.doi.org/10.1146/annurev.micro.52.1.191>.
- Tabita FR, Hanson TE, Li H, Satagopan S, Singh J, Chan S. 2007. Function, structure, and evolution of the RubisCO-like proteins and their RubisCO homologs. *Microbiol Mol Biol Rev* 71:576–599. <http://dx.doi.org/10.1128/MMBR.00015-07>.
- Hugler M, Sievert SM. 2011. Beyond the Calvin cycle: autotrophic carbon fixation in the ocean. *Annu Rev Mar Sci* 3:261–289. <http://dx.doi.org/10.1146/annurev-marine-120709-142712>.
- Hügler M, Wirsén G, Fuchs G, Taylor CD, Sievert SM. 2005. Evidence for autotrophic CO<sub>2</sub> fixation via the reductive tricarboxylic acid cycle by members of the  $\epsilon$  subdivision of *Proteobacteria*. *J Bacteriol* 187:3020–3027. <http://dx.doi.org/10.1128/JB.187.9.3020-3027.2005>.
- Beh M, Strauss G, Huber R, Stetter K-O, Fuchs G. 1993. Enzymes of the reductive citric acid cycle in the autotrophic eubacterium *Aquifex pyrophilus* and in the archaeobacterium *Thermoproteus neutrophilus*. *Arch Microbiol* 160:306–311. <http://dx.doi.org/10.1007/BF00292082>.
- Mehta MP, Butterfield DA, Baross JA. 2003. Phylogenetic diversity of nitrogenase (*nifH*) genes in deep-sea and hydrothermal vent environments of the Juan de Fuca Ridge. *Appl Environ Microbiol* 69:960–970. <http://dx.doi.org/10.1128/AEM.69.2.960-970.2003>.
- Gaby JC, Buckley DH. 2012. A comprehensive evaluation of PCR primers to amplify the *nifH* gene of nitrogenase. *PLoS One* 7:e42149. <http://dx.doi.org/10.1371/journal.pone.0042149>.
- Smith GB, Tiedje JM. 1992. Isolation and characterization of a nitrite reductase gene and its use as a probe for denitrifying bacteria. *Appl Environ Microbiol* 58:376–384.
- Braker G, Fesefeldt A, Witzel K-P. 1998. Development of PCR primer systems for amplification of nitrite reductase genes (*nirK* and *nirS*) to detect denitrifying bacteria in environmental samples. *Appl Environ Microbiol* 64:3769–3775.
- Braker G, Zhou J, Wu L, Devol AH, Tiedje JM. 2000. Nitrite reductase genes (*nirK* and *nirS*) as functional markers to investigate diversity of denitrifying bacteria in Pacific Northwest marine sediment communities. *Appl Environ Microbiol* 66:2096–2104. <http://dx.doi.org/10.1128/AEM.66.5.2096-2104.2000>.
- Bothe H, Jost G, Schlöter M, Ward BB, Witzel K-P. 2000. Molecular analysis of ammonia oxidation and denitrification in natural environments. *FEMS Microbiol Rev* 24:673–690. <http://dx.doi.org/10.1111/j.1574-6976.2000.tb00566.x>.
- Jackson CR, Dugas SL. 2003. Phylogenetic analysis of bacterial and archaeal *arsC* gene sequences suggests an ancient, common origin for arsenate reductase. *BMC Evol Biol* 3:18. <http://dx.doi.org/10.1186/1471-2148-3-18>.

32. Mukhopadhyay R, Rosen BP. 2002. Arsenate reductases in prokaryotes and eukaryotes. *Environ Health Perspect* 110:745. <http://dx.doi.org/10.1289/ehp.02110s5745>.
33. Meyer-Dombard DAR, Amend JP, Osburn MR. 2013. Microbial diversity and potential for arsenic and iron biogeochemical cycling at an arsenic rich, shallow-sea hydrothermal vent (Tutum Bay, Papua New Guinea). *Chem Geol* 348:37–47. <http://dx.doi.org/10.1016/j.chemgeo.2012.02.024>.
34. Wang F, Zhou H, Meng J, Peng X, Jiang L, Sun P, Zhang C, Van Nostrand JD, Deng Y, He Z, Wu L, Zhou J, Xiao X. 2009. GeoChip-based analysis of metabolic diversity of microbial communities at the Juan de Fuca Ridge hydrothermal vent. *Proc Natl Acad Sci U S A* 106:4840–4845. <http://dx.doi.org/10.1073/pnas.0810418106>.
35. Breier JA, Gomez-Ibanez D, Reddington E, Huber JA, Emerson D. 2012. A precision multi-sampler for deep-sea hydrothermal microbial mat studies. *Deep Sea Res Part 1 Oceanogr Res Pap* 70:83–90. <http://dx.doi.org/10.1016/j.dsr.2012.10.006>.
36. Namiki T, Hachiya T, Tanaka H, Sakakibara Y. 2012. MetaVelvet: an extension of Velvet assembler to *de novo* metagenome assembly from short sequence reads. *Nucleic Acids Res* 40:e155. <http://dx.doi.org/10.1093/nar/gks678>.
37. Meyer F, Paarmann D, D'Souza M, Olson R, Glass EM, Kubal M, Paczian T, Rodriguez A, Stevens R, Wilke A, Wilkening J, Edwards RA. 2008. The metagenomics RAST server—a public resource for the automatic phylogenetic and functional analysis of metagenomes. *BMC Bioinformatics* 9:386. <http://dx.doi.org/10.1186/1471-2105-9-386>.
38. Kato S, Nakawake M, Ohkuma M, Yamagishi A. 2012. Distribution and phylogenetic diversity of *cbfM* genes encoding RubisCO form II in a deep-sea hydrothermal field revealed by newly designed PCR primers. *Extremophiles* 16:277–283. <http://dx.doi.org/10.1007/s00792-011-0428-6>.
39. Campbell BJ, Stein JL, Cary SC. 2003. Evidence of chemolithoautotrophy in the bacterial community associated with *Alvinella pompejana*, a hydrothermal vent polychaete. *Appl Environ Microbiol* 69:5070–5078. <http://dx.doi.org/10.1128/AEM.69.9.5070-5078.2003>.
40. Pruesse E, Quast C, Knittel K, Fuchs BM, Ludwig W, Peplies J, Glockner FO. 2007. SILVA: a comprehensive online resource for quality checked and aligned ribosomal RNA sequence data compatible with ARB. *Nucleic Acids Res* 35:7188–7196. <http://dx.doi.org/10.1093/nar/gkm864>.
41. Ludwig W, Strunk O, Westram R, Richter L, Meier H, Kumar Y, Buchner A, Lai T, Steppi S, Jobb G, Förster W, Brettske I, Gerber S, Ginhart AW, Gross O, Grumann S, Hermann S, Jost R, König A, Liss T, Lüßmann R, May M, Nonhoff B, Reichel B, Strehlow R, Stamatakis A, Stuckmann N, Vilbig A, Lenke M, Ludwig T, Bode A, Schleifer K-H. 2004. ARB: a software environment for sequence data. *Nucleic Acids Res* 32:1363–1371. <http://dx.doi.org/10.1093/nar/gkh293>.
42. Moyer CL. 2001. Molecular phylogeny: applications and implications for marine microbiology, p 375–394. *In* Paul JH (ed), *Marine microbiology. Methods in microbiology*, vol 30. Elsevier, St. Petersburg, FL.
43. Ritalahti KM, Amos BK, Sung Y, Wu Q, Koenigsberg SS, Löffler FE. 2006. Quantitative PCR targeting 16S rRNA and reductive dehalogenase genes simultaneously monitors multiple *Dehalococcoides* strains. *Appl Environ Microbiol* 72:2765–2774. <http://dx.doi.org/10.1128/AEM.72.4.2765-2774.2006>.
44. Davis RE, Moyer CL. 2008. Extreme spatial and temporal variability of hydrothermal microbial mat communities along the Mariana Island Arc and southern Mariana back-arc system. *J Geophys Res* 113:B08S15. <http://dx.doi.org/10.1029/2007JB005413>.
45. Von Damm KL, Edmond JM, Grant B, Measures CI, Walden B, Weiss RF. 1985. Chemistry of submarine hydrothermal solutions at 21°N, East Pacific Rise. *Geochim Cosmochim Acta* 49:2197–2220. [http://dx.doi.org/10.1016/0016-7037\(85\)90222-4](http://dx.doi.org/10.1016/0016-7037(85)90222-4).
46. Garside C. 1982. A chemiluminescent technique for the determination of nanomolar concentrations of nitrate and nitrite in seawater. *Mar Chem* 11:159–167. [http://dx.doi.org/10.1016/0304-4203\(82\)90039-1](http://dx.doi.org/10.1016/0304-4203(82)90039-1).
47. Holmes RM, Aminot A, Kérouel R, Hooker BA, Peterson BJ. 1999. A simple and precise method for measuring ammonium in marine and freshwater ecosystems. *Can J Fish Aquat Sci* 56:1801–1808. <http://dx.doi.org/10.1139/f99-128>.
48. Grasshoff K, Kremling K, Ehrhardt M. 2009. *Methods of seawater analysis*, 3rd ed. John Wiley & Sons, Hoboken, NJ.
49. Stookey LL. 1970. Ferrozine—a new spectrophotometric reagent for iron. *Anal Chem* 42:779–781. <http://dx.doi.org/10.1021/ac60289a016>.
50. Clarke K, Gorley RN. 2006. PRIMER v6: user manual/tutorial. Primer-E, Plymouth, United Kingdom.
51. Agrawal A, Lal B. 2009. Rapid detection and quantification of bisulfite reductase genes in oil field samples using real-time PCR. *FEMS Microbiol Ecol* 69:301–312. <http://dx.doi.org/10.1111/j.1574-6941.2009.00714.x>.
52. Henry S, Baudoin E, López-Gutiérrez JC, Martin-Laurent F, Brauman A, Philippot L. 2004. Quantification of denitrifying bacteria in soils by *nirK* gene targeted real-time PCR. *J Microbiol Methods* 59:327–335. <http://dx.doi.org/10.1016/j.mimet.2004.07.002>.
53. Church MJ, Jenkins BD, Karl DM, Zehr JP. 2005. Vertical distributions of nitrogen-fixing phylotypes at Stn ALOHA in the oligotrophic North Pacific Ocean. *Aquat Microb Ecol* 38:3–14. <http://dx.doi.org/10.3354/ame038003>.
54. Rose TM, Schultz ER, Henikoff JG, Pietrokovski S, McCallum CM, Henikoff S. 1998. Consensus-degenerate hybrid oligonucleotide primers for amplification of distantly related sequences. *Nucleic Acids Res* 26:1628–1635. <http://dx.doi.org/10.1093/nar/26.7.1628>.
55. Xie W, Wang F, Guo L, Chen Z, Sievert SM, Meng J, Huang G, Li Y, Yan Q, Wu S, Wang X, Chen S, He G, Xiao X, Xu A. 2011. Comparative metagenomics of microbial communities inhabiting deep-sea hydrothermal vent chimneys with contrasting chemistries. *ISME J* 5:414–426. <http://dx.doi.org/10.1038/ismej.2010.144>.
56. Bourbonnais A, Juniper SK, Butterfield DA, Devol AH, Kuypers MMM, Lavik G, Hallam SJ, Wenk CB, Chang BX, Murdock SA, Lehmann MF. 2012. Activity and abundance of denitrifying bacteria in the subsurface biosphere of diffuse hydrothermal vents of the Juan de Fuca Ridge. *Biogeosci Discuss* 9:4177–4223. <http://dx.doi.org/10.5194/bgd-9-4177-2012>.
57. Singer E, Heidelberg JF, Dhillon A, Edwards KJ. 2013. Metagenomic insights into the dominant Fe(II) oxidizing *Zetaproteobacteria* from an iron mat at Loihi, Hawaii. *Front Microbiol* 4:52. <http://dx.doi.org/10.3389/fmicb.2013.00052>.
58. Minic Z, Thongbam PD. 2011. The biological deep sea hydrothermal vent as a model to study carbon dioxide capturing enzymes. *Mar Drugs* 9:719–738. <http://dx.doi.org/10.3390/md9050719>.
59. Wheat CG, Jannasch HW, Plant JN, Moyer CL, Sansone FJ, McMurtry GM. 2000. Continuous sampling of hydrothermal fluids from Loihi Seamount after the 1996 event. *J Geophys Res* 105:19353–19367. <http://dx.doi.org/10.1029/2000JB900088>.
60. Campbell BJ, Engel AS, Porter ML, Takai K. 2006. The versatile  $\epsilon$ -proteobacteria: key players in sulphidic habitats. *Nat Rev Microbiol* 4:458–468. <http://dx.doi.org/10.1038/nrmicro1414>.
61. Feely RA, Trefry JH, Massoth GJ, Metz S. 1991. A comparison of the scavenging of phosphorus and arsenic from seawater by hydrothermal iron oxyhydroxides in the Atlantic and Pacific Oceans. *Deep Sea Res A* 38:617–623. [http://dx.doi.org/10.1016/0198-0149\(91\)90001-V](http://dx.doi.org/10.1016/0198-0149(91)90001-V).
62. Pichler T, Veizer J, Hall GEM. 1999. Natural input of arsenic into a coral-reef ecosystem by hydrothermal fluids and its removal by Fe(III) oxyhydroxides. *Environ Sci Technol Lett* 33:1373–1378. <http://dx.doi.org/10.1021/es980949+>.
63. Breier JA, Toner BM, Fakra SC, Marcus MA, White SN, Thurnherr AM, German CR. 2012. Sulfur, sulfides, oxides and organic matter aggregated in submarine hydrothermal plumes at 9°50'N East Pacific Rise. *Geochim Cosmochim Acta* 88:216–236. <http://dx.doi.org/10.1016/j.gca.2012.04.003>.
64. Smith CJ, Osborn AM. 2009. Advantages and limitations of quantitative PCR (Q-PCR)-based approaches in microbial ecology. *FEMS Microbiol Ecol* 67:6–20. <http://dx.doi.org/10.1111/j.1574-6941.2008.00629.x>.